**ORIGINAL ARTICLE**

# Total-body $^{18}$F-FDG PET/CT scan in oncology patients: how fast could it be?

Pengcheng Hu[1,2,3] · Yiqiu Zhang[1,2,3] · Haojun Yu[1,2,3] · Shuguang Chen[1,2,3] · Hui Tan[1,2,3] · Chi Qi[1,2,3] · Yun Dong[4] · Ying Wang[4] · Zilin Deng[4] · Hongcheng Shi[1,2,3]

## Abstract

**Purpose** The aim of the study was to determine a faster PET acquisition protocol for a total-body PET/CT scanner by assessing the image quality that is equivalent to a conventional digital PET/CT scanner from both a phantom and a clinical perspective.

**Methods** A phantom study using a NEMA/IEC NU-2 body phantom was first performed in both a total-body PET/CT (uEXPLORER) and a routine digital PET/CT (uMI 780), with a hot sphere to background activity concentration ratio of 4:1. The contrast recovery coefficient (CRC), background variability (BV), and recovery coefficient (RC: $RC_{max}$ and $RC_{mean}$) were assessed in the uEXPLORER with different scanning durations and reconstruction protocols, which were compared to those acquired from the uMI 780 with clinical acquisition settings. The coefficient of variation (COV) of the uMI 780 with clinical settings was calculated and used as a threshold reference to determine the optimized scanning duration and reconstruction protocol for the uEXPLORER. The obtained protocol from the phantom study was subsequently tested and validated in 30 oncology patients. Images acquired from the uMI 780 with 2–3 min per bed position were referred as G780 and served as the reference for comparison. All PET raw data from the uEXPLORER were reconstructed using the data-cutting technique to simulate a 30-s, 45-s, or 60-s acquisition duration, respectively. The iterations were 2 and 3 for the uEXPLORER, referred as G30s_3i, G45s_2i, G45s_3i, G60s_2i, and G60s_3i, respectively. A 5-point Likert scale was used in the qualitative analysis to assess the image quality. The image quality was also evaluated by the liver COV, the lesion target-to-background ratio (TBR), and the lesion signal-to-noise ratio (SNR).

**Results** In the phantom study, CRC, BV, $RC_{max}$, and $RC_{mean}$ in the uEXPLORER with different scanning durations and reconstruction iterations were compared with those in the uMI 780 with clinical settings. A minor fluctuation was found among different scanning durations. COV of the uMI 780 with clinical settings was 11.6%, and a protocol with a 30–45-s scanning duration and 2 or 3 iterations for the uEXPLORER was found to provide an equivalent image quality as the uMI 780. An almost perfect agreement was shown with a kappa value of 0.875. The qualitative score of the G30s_3i in the uEXPLORER was inferior to the G780 reference ($p = 0.001$); however, the scores of other groups in the uEXPLORER with a 45-s and above acquisition time were higher than the G780 in the uMI 780. In quantitative analysis, the delay time between the two scans in the two orders was not significantly different. There was no significant difference of the liver COV between the G780 and G30s_3i ($p = 0.162$). A total of 33 lesions were analyzed in the clinical patient study. There was no significant difference in lesion TBR between the reference G780 and the G45s_2i obtained from the uEXPLORER ($p = 0.072$), while the latter showed a higher lesion SNR value compared to that in uMI 780 with clinical settings ($p < 0.001$).

**Conclusions** This study showed that a fast PET protocol with a 30–45-s acquisition time in the total-body uEXPLORER PET/CT can provide an equivalent image quality as the conventional digital uMI 780 PET/CT with longer clinical acquisition settings.

---

Pengcheng Hu and Yiqiu Zhang contributed equally to this work.

This article is part of the Topical Collection on Oncology - General

✉ Hongcheng Shi
shi.hongcheng@zs-hospital.sh.cn

[1] Department of Nuclear Medicine, Zhongshan Hospital, Fudan University, 180 Fenglin Road, Shanghai 200032, China

[2] Nuclear Medicine Institute of Fudan University, Shanghai 200032, China

[3] Shanghai Institute of Medical Imaging, Shanghai 200032, China

[4] United Imaging Healthcare Co., Ltd., Shanghai, China

## Introduction

Positron emission tomography and computed tomography (PET/CT) is widely used for staging, restaging, and therapy response assessment in oncology [1–7]. Efforts have been made over the past years to improve PET performance, by implementing the fast scintillator (lutetium oxyorthosilicate, LSO), solid-state silicon photomultiplier (SiPM), time of flight (TOF), point spread function (PSF) reconstruction, and extension of the axial field of view (AFOV) [8–16].

The state-of-the-art PET/CT, total-body PET/CT scanner (uEXPLORER, United Imaging Healthcare, China), implements all the above improvements with an AFOV up to 194 cm. The total-body PET scanner has a very high sensitivity of 176 kcps/MBq, a count rate performance with a peak noise equivalent count rate (NECR) of approximately 2 Mcps, and a good spatial resolution capability for human imaging ($\leq$ 2.9 mm FWHM near the center of the AFOV) [17]. This total-body PET/CT scanner has been used in the clinical practice with a superior performance, compared to other routine PET/CT scanners in our site. Given its high sensitivity, a faster scan protocol is feasible with a shortened PET acquisition by a factor of even up to 40× theoretically [18]. A faster PET scan can greatly improve patient comfort, especially for those who cannot lie steadily for 10–20 min. Moreover, a faster PET scan can be applied in other scenarios, such as a single breath-hold PET acquisition for lung cancer. However, it is unknown how short the acquisition can be to achieve an equivalent image quality as that in routine practice. To the best of our knowledge, such a comparison based on both a phantom and clinical study has not been performed yet. A recent commercially available digital PET/CT (uMI 780, United Imaging Healthcare, China) was selected as a routine PET/CT scanner for comparison in the study. It is a "miniature" version of the total-body PET/CT with a limited AFOV of 30 cm, with the same techniques implemented except for the extended AFOV. It has a spatial resolution of 2.9 mm, sensitivity of 16.0 cps/kBq, peak NECR activity of 200 kcps, and a TOF resolution of 430 ps [19].

In the first part of the study, a phantom with known geometry and activity preparation was used to assess the image quality of the two PET scanners.

The National Electrical Manufacturers Association (NEMA)/International Electrotechnical Commission (IEC) NU-2 phantom, which has been commonly used in PET studies to simulate the patient morphology and tracer distribution [20, 21], was used in the current inter-scanner study. We compared background variability (BV), recovery coefficients (RCs), and contrast recovery coefficient (CRC) in the uEXPLORER with different scanning durations and reconstruction protocols to those in the reference uMI 780 protocol used in our clinical practice. The coefficient of variation (COV) was compared between the two machines to determine an optimized protocol for an equivalent image quality. In the subsequent clinical study, the optimized protocol was tested and validated in an enrolled cohort of oncology patients.

The aim of the study was to determine a faster PET acquisition protocol for the total-body uEXPLORER scanner by assessing the image quality that is equivalent to the uMI 780 digital PET/CT scanner both from a phantom and clinical perspective.

## Methods

### Phantom study

#### Phantom preparation

In the phantom study, a NEMA/IEC NU-2 phantom was used to test the small lesion detectability and contrast recovery versus background noise in $^{18}$F-FDG PET/CT images of the two PET/CT scanners [22]. The phantom has six spherical inserts with 10, 13, 17, 22, 28, and 37 mm in diameter. In addition, a 16-cm-long cylinder lung insert with a diameter of 5 cm was positioned in the center of the phantom to simulate the lung tissue attenuation. To simulate the average hepatic activity concentration in patients who underwent $^{18}$F-FDG PET imaging 60 min after a weight-based administration of 3.7 MBq/kg, the phantom was filled with a background activity concentration of 2.65 kBq/mL, which was ensured at the start of data acquisition. The radioactivity concentration ratio of the background to all the six spheres was 1:4 [23]. The phantom was prepared following the same procedure on a different day for the acquisition on the other PET/CT scanner.

#### Phantom acquisition and reconstruction

The phantom was placed horizontally on the bed to make sure the hot spheres were localized at the center of axial field of view in the uMI 780 and the center of unit 2 in the uEXPLORER. Then, a CT scan was first acquired for attenuation correction, followed by an emission scan with 10 min in both the scanners. Images in the uMI 780 were reconstructed with clinical settings. PET reconstruction was performed with 2-min duration using TOF + PSF, subsets = 20, iteration = 2, image matrix = 150 × 150, FOV = 500, and the full width at half maximum (FWHM) of the Gaussian filter function of 3 mm.

To compare the clinical PET/CT images of the uEXPLORER with the routine uMI 780 with clinical settings, reconstructions were performed using time subsets of 0.3, 0.5, 0.68, 1, 1.36, 2.04, 2.72, 4.09, 5.46, and 6.38 min from the original 10-min data with normalization, system dead time, random, scatter, and attenuation correction. The reconstruction was performed using TOF + PSF, subsets = 20, iteration = 2 and 3, matrix = 192 × 192, FOV = 600, and the FWHM of the Gaussian filter function of 3 mm.

## Phantom data analysis

For each set of the images from the two scanners, three rectangular regions of interests (ROIs), with an area of 900 mm$^2$, were drawn on the three central transverse image slices (Fig. 1). The noise was determined by dividing the standard deviation to the mean pixel value for each ROI. The image coefficient of variation (COV) for a reconstructed image was acquired by averaging the values in the nine ROIs. A COV < 15% was considered an acceptable noise level as suggested in the EARL procedure [24, 25].

For sphere characterization, a cubic volume of interest (side of 50 mm) was placed on each sphere of the phantom as shown in Fig. 2 [24]. The maximum RCs of all the spheres were obtained as in the EANM guidelines for tumor PET imaging [20, 26]. The mean RCs were derived with additional spherical VOIs, matching the actual insert volume. Furthermore, the corresponding contrast recovery coefficients

(CRC) were analyzed according to the NEMA NU-2 2018 standard [22].

In this study, the COV, RCs, and CRC with a routine 2-min scanning duration in the uMI 780 with clinical settings were used as the reference. To compare the image noise with that in the reference, a graph was plotted to compare the COVs with different scanning durations in the uEXPLORER. The optimized scanning duration and reconstruction parameters in the uEXPLORER were determined when the noise was consistent with that in the uMI 780 with clinical settings. Then, in the subsequent clinical study, the reconstructions were performed with the optimized scanning duration and the proposed parameters for the uEXPLORER. Compared to that in the uMI 780 with clinical settings, the image quality with optimized scanning duration and reconstruction parameters in the uEXPLORER was subsequently validated.

It should be noted that there were different image matrices, FOVs, pixel sizes, and iterations used in the image reconstruction in both the phantom and clinical study for the two scanners according to the clinical practice in our site.

## Clinical study

### Patients

Forty consecutive patients, referred for cancer staging or restaging in our hospital, were prospectively recruited in the



**Fig. 1** Region of interest (ROI) analysis on images of the NEMA/IEC body phantom in the uMI780 (**a**, **b**) and uEXPLORER (**c**, **d**). The subfigures of **a** and **c** show locations of the circular ROIs for the six hot spheres; and **b** and **d** show the three 900-mm$^2$ rectangular ROIs for background COV analysis. The ROIs of the uMI780 were placed in the same positions as the uEXPLORER
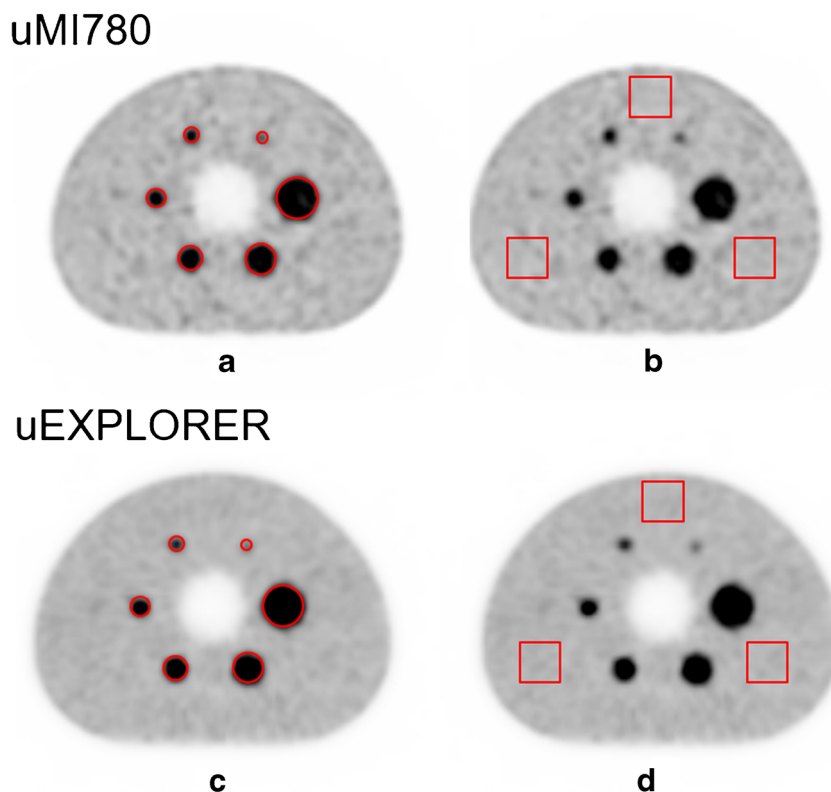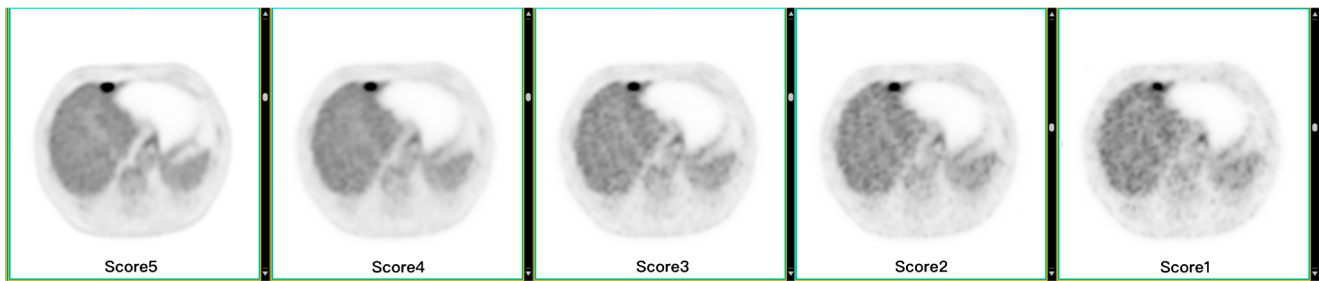
**Fig. 2** An illustration of the 5-point Likert score for qualitative assessment of the image quality (5 to 1 from the left to the right, respectively). Where 1 = unacceptable image quality for diagnosis, 2 = acceptable image quality with no need to repeat the scan, 3 = fair image quality as in the routine practice, 4 = good image quality with performance excessed the routine practice, and 5 = excellent image quality

study. In order to minimize the impact induced by the delayed time between the two scans, studies with a time difference longer than 40 min were excluded from the study. In total, ten studies were excluded because of the long delay time and other technical issues (motion artifacts and the difference in the scan order). A total of 30 patients were finally enrolled (10/20 female/male, age 64.2 ± 9.3 years) with diagnoses of lung cancer ($n = 3$), gastric cancer ($n = 5$), esophageal cancer ($n = 3$), liver cancer ($n = 3$), bile duct cancer ($n = 1$), duodenal cancer ($n = 1$), pancreatic cancer ($n = 2$), colon cancer ($n = 5$), and rectal cancer ($n = 7$). The demographic and clinical characteristics of the enrolled patients are listed in Table 1.

The study was approved by the Institutional Review Board of Shanghai Zhongshan Hospital affiliated to Fudan University, and a written consent form was signed by the patients prior to the scan.

## Clinical PET/CT imaging and reconstruction

All patients have fasted for at least 6 h before the injection of $^{18}$F-FDG. The blood glucose level of patients was under

**Table 1** Patient demographic and clinical information

| Characteristic | Data |
| --- | --- |
| Age (years) | 64.2 ± 9.3 [37, 79][*] |
| Sex (female/male) | 10/20 |
| Weight (kg) | 62.9 ± 9.5 [40.8, 78.1][*] |
| Height (cm) | 163.7 ± 8.0 [148.0, 183.1][*] |
| BMI (kg/m$^2$) | 23.4 ± 2.9 [18.1, 30.4] |
| Injected dose (MBq) | 227.9 ± 34.9 [149.5, 289.7][*] |
| Injected dose per weight (MBq/kg) | 3.62 ± 0.17 [3.34, 3.95][*] |
| Uptake time of uMI 780 in uMI780-first group (min) | 72 ± 15 [53, 104][*] |
| Uptake time of uEXPLORER in uMI780-first group (min) | 98 ± 17 [76, 103][*] |
| Uptake time of uMI 780 in uMI780-second group (min) | 87 ± 20 [60, 129][*] |
| Uptake time of uEXPLORER in uMI780-first group (min) | 67 ± 18 [40, 104][*] |
| Delayed time between two PET scans (min) | 24 ± 28 [10, 39][*] |
| Location of the primary lesion | |
|   Lung | 3[+] |
|   Esophagus | 3[+] |
|   Liver | 3[+] |
|   Stomach | 5[+] |
|   Pancreas | 2[+] |
|   Bile duct | 1[+] |
|   Duodenum | 1[+] |
|   Colon | 5[+] |
|   Rectum | 7[+] |

[*] Data were presented as mean ± SD [range]

[+] Indicated the number of the patients

11 mmol/L before the injection. After a single radiotracer injection of ^{18}F-FDG (3.7 MBq/kg), all patients underwent two PET/CT scans, on a routine digital PET/CT scanner (uMI 780, United Imaging Healthcare, China) and a total-body PET/CT scanner (uEXPLORER, United Imaging Healthcare, China). With an uptake of approximately 60 min after the injection, 15 patients were first scanned with the uEXPLORER, followed by a second scan with the uMI 780. In the remaining 15 patients, the scans were performed with an alternative order. The average uptake time was $84 \pm 23$ min for the uEXPLORER, and $79 \pm 19$ min for the uMI 780. Time delay between two scans was controlled under 40 min with a mean value of $24 \pm 8$ min.

The CT subsystems of both scanners consist of a 160-slice detector. A diagnostic CT was performed in the first scan with 120 kVp tube current modulation, spiral pitch factor of 0.9875, slice thickness of 1 mm, and slice increment of 1 mm. No intravenous or oral contrast was used. A low-dose CT acquisition (120 kVp, 9 mAs, spiral pitch factor of 1.10125, 1.4-mm slice thickness with slice increment of 3.0 mm) for attenuation correction was used in the second scan in order to minimize the radiation exposure to the patients.

As in our clinical practice, PET was acquired in the uMI 780 with 2–3 min for each bed position covering the lung, abdomen, and pelvic region. The total PET acquisition was about 10–13 min for the body part with an additional 3 min for the head. In the uEXPLORER, PET was acquired in one bed position to cover the entire patient body with a total acquisition time of 5 min in the study. All PET raw data were stored in list mode, and reconstructions were performed using the data-cutting technique to simulate a 30-s, 45-s, or 60-s acquisition duration in the uEXPLORER. Both the reconstructions were performed with the following parameters as determined in the phantom study: an FOV of 600, a matrix of $192 \times 192$, 20 subsets, and an FWHM of the Gaussian filter function of 3 mm. The iterations were 2 and 3 for the uEXPLORER, referred as G30s_3i, G45s_2i, G45s_3i, G60s_2i, and G60s_3i, respectively. The standard corrections, including decay, random, dead time, attenuation, and normalization correction, were applied in all of the PET reconstructions. In addition, the point spread function (PSF) and time of flight (TOF) were also used to reconstruct the images. However, due to the system configuration, the slice thickness was slightly different, as in the phantom study.

## Clinical image analysis

The image quality was qualitatively assessed by two experienced nuclear medicine physicians with over 10-year experience in interpreting PET/CT images on a dedicated workstation (uMI, United Imaging Healthcare, China). A 5-point Likert scale was used to score the overall image quality with 1 = unacceptable image quality for diagnosis, 2 = acceptable image quality with no need to repeat the scan, 3 = fair image quality as in the routine practice, 4 = good image quality with performance excessed the routine practice, and 5 = excellent image quality (Fig. 2).

The PET image was then assessed by a technician supervised by an experienced nuclear medicine physician. For PET images of each patient, a circular region of interest (ROI) with a diameter of $20 \pm 2$ mm was manually drawn in the homogeneous region of the liver away from the edges and lesions. $SUV_{max}$, $SUV_{mean}$, and SD were measured and recorded. Liver COV was obtained by the following equation, and used as a measure of the image noise (Eq. 1).

$$COV = \frac{liverSD}{liverSUV_{mean}} \tag{1}$$

For each patient, the lesions with a diameter less than 40 mm were selected in the study according to the sphere size in the phantom study. For each patient, two lesions (if there were) were selected in <10 mm, 10–20 mm, and 20–40 mm groups, respectively. The lesion uptake was measured by drawing a volume of interest (VOI) with a threshold of 50% of the $SUV_{max}$ value within the contour margin. Both $SUV_{max}$ and $SUV_{mean}$ of the lesion were measured. The target-to-background ratio (TBR) and signal-to-noise ratio (SNR) were calculated by the following equations and were used as a measure of lesion contrast (Eq. 2 and Eq. 3).

$$TBR = \frac{lesionSUV_{max}}{liverSUV_{mean}} \tag{2}$$

$$SNR = \frac{lesionSUV_{mean} - liverSUV_{mean}}{liverSD} \tag{3}$$

## Statistical analysis

Continuous parameters were presented as mean and standard deviation. Cohen's kappa test was used to compare the inter-reader agreement and Wilcoxon signed-rank test was used to compare the subjective scores between the uEXPLORER groups and G780 group. The delay time between the two scan orders was compared with independent $t$ test. Paired $t$ test was performed to compare the quantitative parameters between the two scanners.

A $p$ value <0.05 was considered significant. Statistical analysis was performed with SPSS version 25.0 (SPSS Inc., IBM Corporation, Chicago, IL, USA).
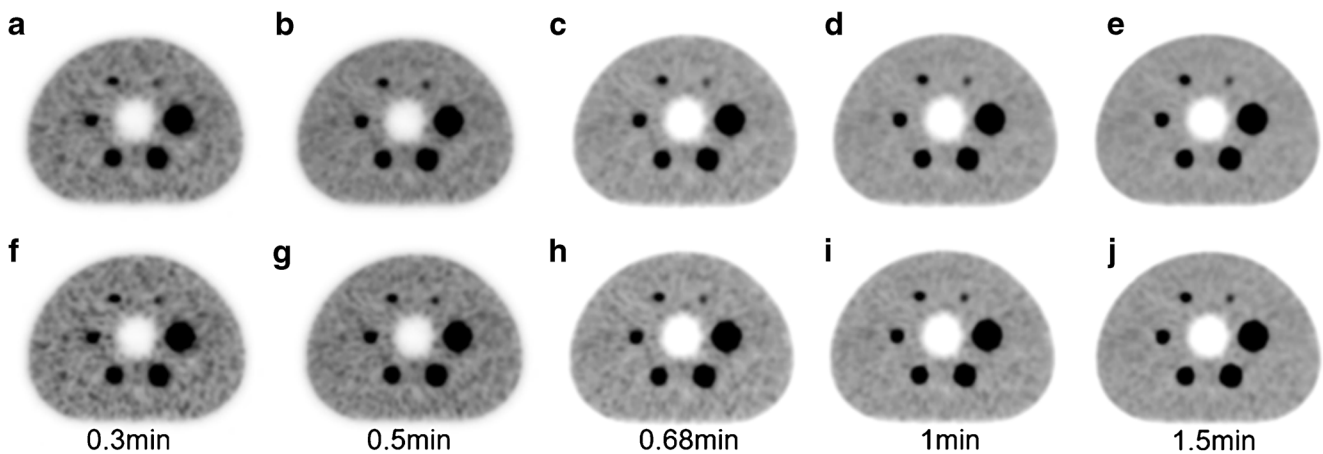
**Fig. 3** Comparison of transverse views of the NEMA/IEC body phantom images of the uEXPLORER, with different OSEM iteration numbers and scan durations. The first row (**a-e**) shows results of iteration number of 2, and the second row (**f-j**) for iteration number of 3. The subplot images in the column from left to right were obtained by using scanning duration of 0.3 (**a, f**), 0.5 (**b, g**), 0.68 (**c, h**), 1.0 (**d, i**), and 1.5 min (**e, j**), respectively. All images were reconstructed with 20 subsets

## Results

### NEMA/IEC body phantom study

Figure 3 shows the transaxial views across the equatorial plane of the various spheres of the phantom, with a scanning duration of 0.3, 0.5, 0.68, 1.0, and 1.5 min in the uEXPLORER. The same dose calibrator and isotope phantom were used in daily quality control for the two PET/CT scanners. The system cross-calibration in background SUV was within the range of 0.95–1.05.

The measured COV as a function of the scanning duration for the uEXPLORER is reported in Fig. 4, where the dashed black line indicated a COV of 11.6% in the uMI 780 with clinical settings. As expected, image noise decreased with the increased scanning duration and increased number of iterations. By a power-law fitting with the COV and scanning duration, the minimal scanning duration was found to be about 30s for the uEXPLORER, where the background variability was similar to that in the uMI 780 with clinical settings.

Figures 5, 6 show the CRC, RCs, and background variability check for the clinical scanning and reconstruction protocol in the uMI 780 and the optimized scanning and reconstruction protocols in the uEXPLORER, respectively. It showed that CRC had a minor fluctuation among the images with a scanning duration of 30, 45, and 60s. Both CRC and BV increased with the increased number of iterative reconstruction. For all the spheres, the uEXPLORER showed a slightly higher CRC for all the time frames than the uMI 780 for both iteration of 2 and 3. The $RC_{max}$ and $RC_{mean}$ for all the spheres in both the PET/CT scanners were almost within the EARL limits. Table 2 shows the optimized scanning and reconstruction protocols in the uEXPLORER which had equivalent image quality with that in the uMI 780.
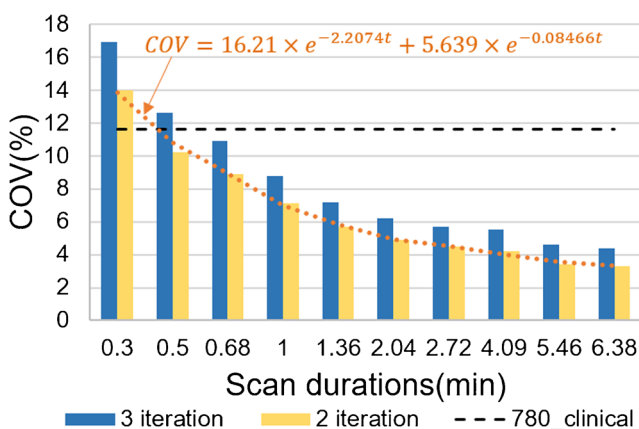
### Clinical validation

The overall inter-reader agreement of the image quality showed a kappa of 0.875, indicating an almost perfect



**Fig. 4** A COV analysis on the body phantom image of the uEXPLORER for different scan durations and different OSEM iterations. The black dashed line (11.6%) is the COV measurement of the uMI780 with clinical protocol for the same phantom. The orange dotted line is a fitted curve for COV (iteration = 2) value as a function of scan duration $t$ (min)

$$COV = 16.21 \times e^{-2.2074t} + 5.639 \times e^{-0.08466t}$$

**Table 2** Optimized reconstruction protocol with uMI 780 and uEXPLORER

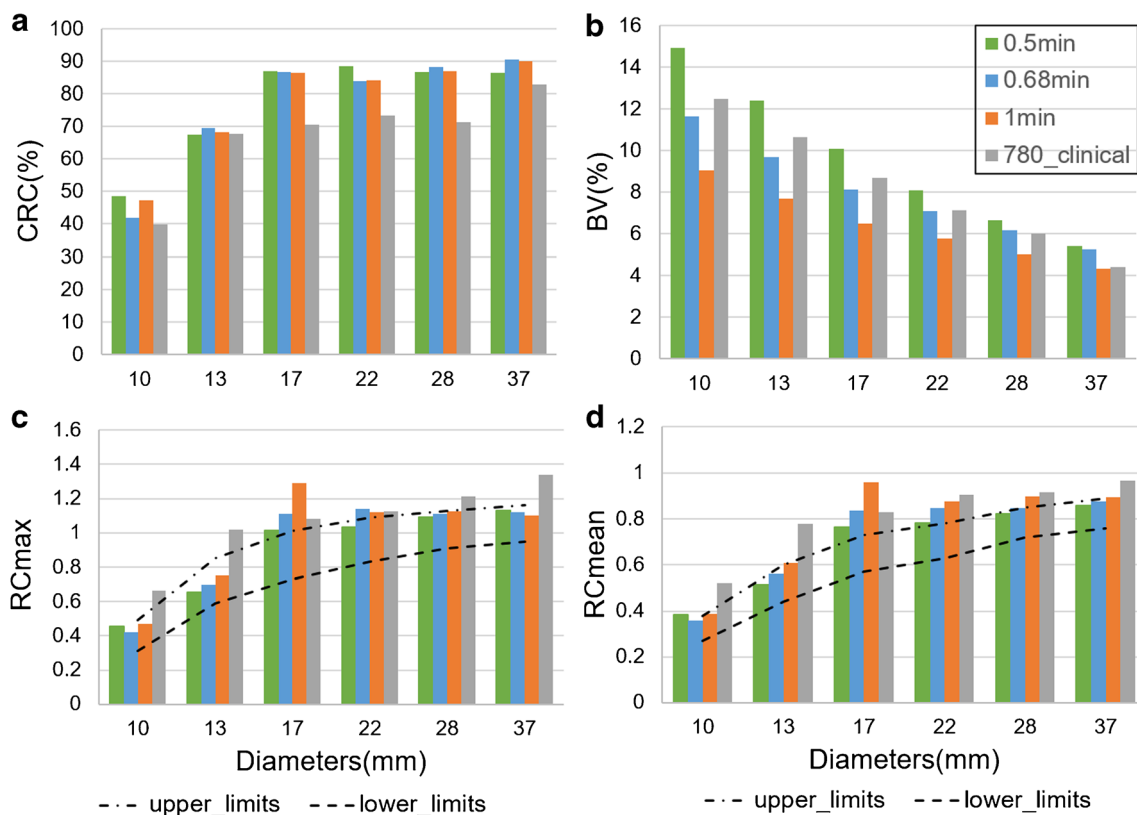|  | uMI780 | uEXPLORER |
|---|---|---|
| Scanning duration/bed (min) | 2 | 0.5/0.75/1 |
| Reconstruction | OSEM+TOF+PSF | OSEM+TOF+PSF |
| Subsets | 20 | 20 |
| FOV/matrix | 500/150×150 | 600/192×192 |
| Slice thickness (mm) | 1.34 | 1.443 |
| Iteration | 2 | 2/3 |

**Fig. 5** CRC (**a**), BV (**b**), RC$_{max}$ (**c**), and RC$_{mean}$ (**d**) analyses on the body phantom images of the uEXPLORER (by 2 iterations) in comparison with the uMI780 with clinical protocol. In all four subfigures, the green, blue, and orange bars are for results of 0.5, 0.68, and 1.0-min scan durations in the uEXPLORER, respectively; the gray ones are for results of the uMI780. The CRC and BV were measured based on the NEMA2018 guidelines. In subfigure (**c**) and (**d**), the dash-dotted and dashed lines were the upper and lower limits suggested by the EANM guideline

agreement between the two readers. The average scores of the two readers for the protocols are listed in Table 3. The subjective score in G780 was significantly higher than that in G30s_3i ($p = 0.001$) and slightly lower than that in the G45s_3i ($p = 0.18$). The other groups in the uEXPLORER with a 45-s and above acquisition time showed a significant higher score than that in the uMI 780.

In the semiquantitative analysis, the delay time between the two scans in the two orders was not significantly different ($p = 0.054$), with a mean value of $26 \pm 7$ min and $21 \pm 8$ min, respectively. There was no significant difference in COV between the G30s_3i and G780 ($p = 0.162$), indicating a consistent image noise in the liver. All the other groups showed a significantly lower COV value than the G780 ($p < 0.001$, Fig. 7). The groups with a longer acquisition showed a lower COV value, and illustrated a better image noise. According to the OSEM algorithm characteristics, the image noise increased as the iteration increased for the groups with the same acquisition. However, all the groups presented a COV value less than 15%, indicating a preferred image noise in the clinical routine (Fig. 8).

A total of 33 lesions were analyzed in the study. For the lesions, there was no significant difference in TBR between the G45s_2i and G780 ($p = 0.072$), indicating a consistent lesion conspicuousness (Fig. 9). As shown in Fig. 10, the two reconstructed images resulted in minor visual variations in lesion contrast. All the other groups showed a significantly higher TBR value than the G780 ($p < 0.001$). In addition, all groups in the uEXPLORER showed a larger SNR value than that in the G780 group ($p < 0.001$, Fig. 9).

## Discussion

With the advent of the uEXPLORER scanner, PET/CT scan has evolved to a total-body imaging in clinics. Its superior performance has made it a powerful tool in oncological applications [18, 19, 27, 28]. The ultra-high sensitivity provides the feasibility of a fast PET scan in routine practice with an improvement in patient comfort and an increased throughput. This study assessed the image quality from the phantom and clinical perspectives to explore a faster PET scan protocol for the uEXPLORER without compromising the image quality compared to a routine digital PET scanner. The PET acquisition using a routine PET/CT scanner in a step-and-shoot mode takes about 10–20 min for the body part and an additional
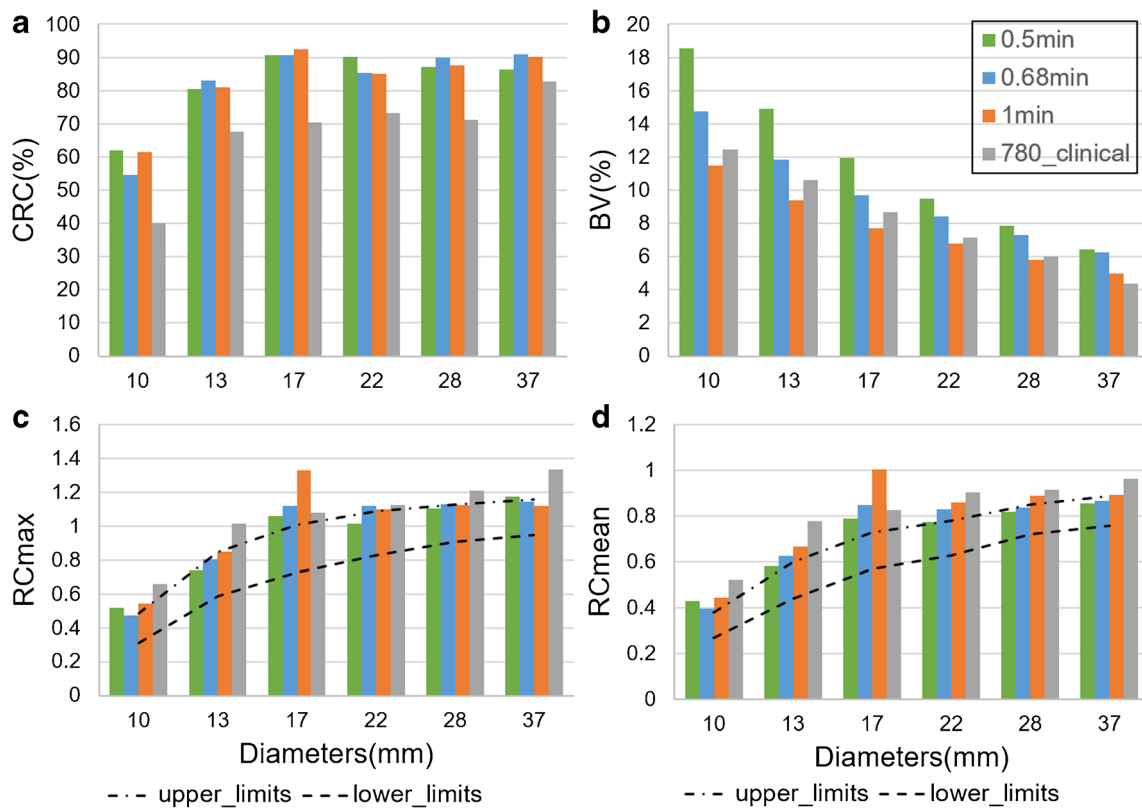
**Fig. 6** CRC (**a**), BV (**b**), $RC_{max}$ (**c**), and $RC_{mean}$ (**d**) analyses on the body phantom images of the uEXPLORER (by 3 iterations) in comparison with the uMI780 with the clinical protocol. The legend and caption in this figure are the same as in Fig. 5

~3 min for the head to cover the scan range from the skull to the mid-thigh. However, in the total-body PET/CT scanner with an AFOV of 194 cm, the PET acquisition can be performed with only one bed position to cover the entire patient body. The study demonstrated a fast PET scan with 30–45-s acquisition can provide an equivalent image quality according to the phantom study and the intra-individual comparison in 30 oncology patients. Furthermore, the study can be potentially regarded as a methodology for an inter-scanner comparison, even for a multi-center study. PET/CT plays an important role in timely monitoring of therapeutic responses in various diseases, such as lymphoma, where multiple PET/CT scans are needed [4]. Multiple PET/CT scans for a certain patient in the

inter-scanner studies always require a consistent image quality to improve the accuracy of the assessment. Therefore, the standardization and optimization of $^{18}$F-FDG protocols are essential in inter-scanner studies as illustrated in the study.

**Table 3** Subjective score in different groups

| Group | Subjective score |
|---|---|
| G780 | 2.95 ± 0.22 |
| G30s_3i | 2.80 ± 0.40* |
| G45s_2i | 3.19 ± 0.55* |
| G45s_3i | 3.03 ± 0.50 |
| G60s_2i | 3.28 ± 0.48* |
| G60s_3i | 3.20 ± 0.54* |

Data were presented as mean ± SD

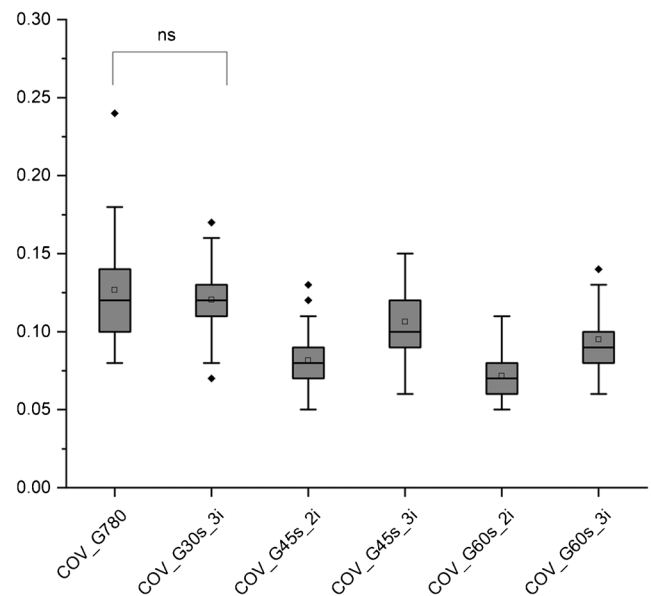*Indicated a significant difference compared to uMI 780



**Fig. 7** COV comparison between clinical groups in the uEXPLORER and uMI 780. There was no significant difference between the G30s_3i and G780. A significant lower COV value was found in the 45-s and above groups than that in the G780 group ($p < 0.001$)

**Fig. 8** Transverse PET images of a 73-year-old woman underwent a total-body PET/CT (**a**) using the uEXPLORER and a subsequent whole PET/CT examination (**b**) using the uMI780. The PET image of the uEXPLORER was reconstructed with 3 iterations and an acquisition of 30s, while the PET image of the uMI780 was reconstructed with the clinical protocol with a 3-min acquisition. Both images showed a preferred image noise
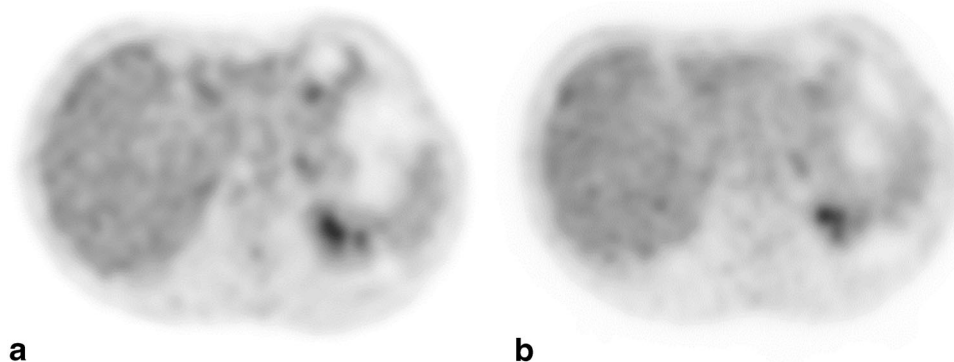


In this study, phantom-based study was performed with a standard NEMA/IEC NU-2 phantom. The phantom was selected since it is a simulation of the patient's morphology and tracer distribution and commonly used in the image quality assessment of PET studies. However, in whole-body or total-body PET studies, the scan range of the patients, either from the skull to the mid-thigh or from the skull to the feet, was much larger than the phantom height. For the total-body PET scans with the uEXPLORER, the patient's body was scanned with different parts of the PET detector along the AFOV. During the design of the phantom study, the limited axial coverage of this phantom has been considered. Because of the consistent sensitivity of the PET scanners along the AFOV of the uEXPLORER [17], the image quality of the patient body can be regarded uniform. Therefore, the standard NEMA/IEC NU-2 phantom was used to assess the image quality in the total-body PET studies.

In the clinical part, the patients were randomly enrolled in the study without strict exclusion criteria, such as age, preparation during the uptake, diabetes, patient size, and cancer type. The enrolled patient group can be regarded as an epitome of the clinical practice. The enrolled patients in the study included almost all the common cancer types where the lesion uptake $SUV_{max}$ varies from 1.0 to 40. The body mass index (BMI), known as an impact factor on the image quality [29, 30], of the enrolled patients varied in a large range (from 18.1 to 30.4). In addition, they were found to have accompanying diseases other than cancer, such as liver cirrhosis, ascites, or with complication of systemic inflammation. Thus, the results of the study indicated a high compatibility and feasibility in the clinical practice.

Furthermore, the reference protocol in the uMI 780 was a typical clinical protocol used in our hospital, with a compromise of the image quality and patient throughput. Although
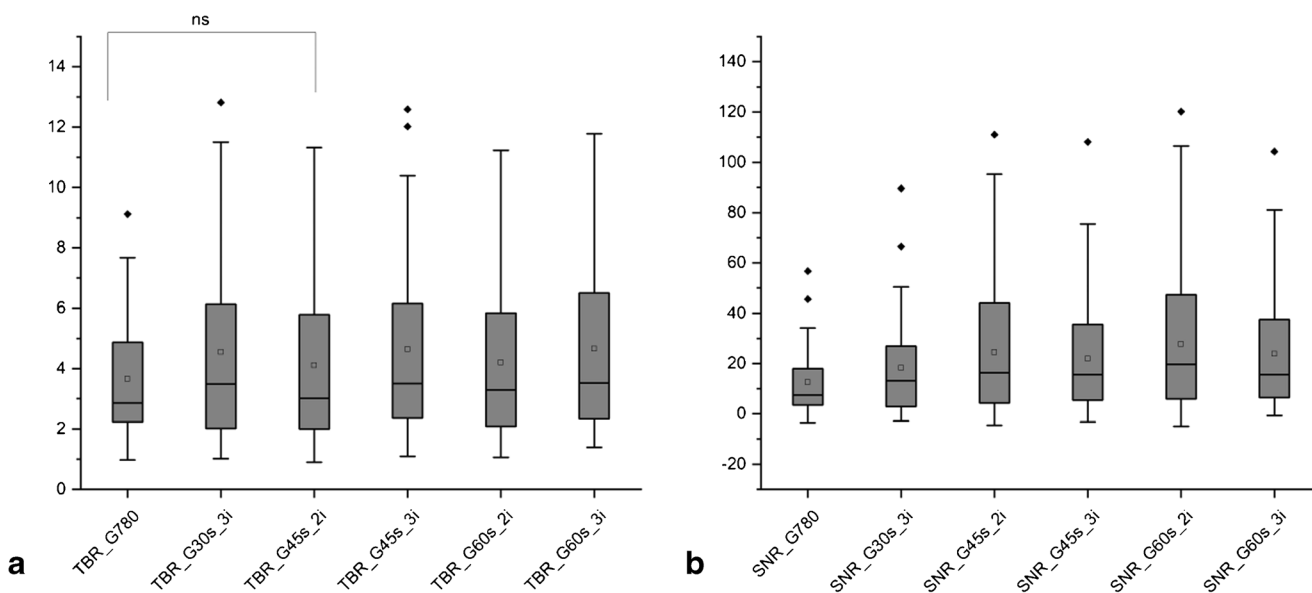


**Fig. 9** TBR and SNR comparison between groups in the uEXPLORER and uMI 780. There was no significant difference in lesion TBR between the G45s_2i and G780. A significant higher TBR value was found in other groups of the uEXPLORER than that in the G780 group (**b**,

$p < 0.001$). All the groups in the uEXPLORER showed a significant higher SNR than the G780 group (**a**, $p < 0.001$). TBR = target-to-background ratio; SNR = signal-to-noise ratio; ns = no significant difference

**Fig. 10** PET transverse and MIP images of a 64-year-old woman diagnosed with hepatocellular carcinoma(HCC). A total-body PET/CT imaging was performed first (**c, d**) in the uEXPLORER with a subsequent whole-body PET/CT (**a, b**) in the uMI 780. Subfigures **a** and **b** were reconstructed with the clinical protocol, and **c** and **d** with 2 iterations and a 45-s acquisition. Both the transverse and coronal images show a good lesion contrast which can meet clinical requirements
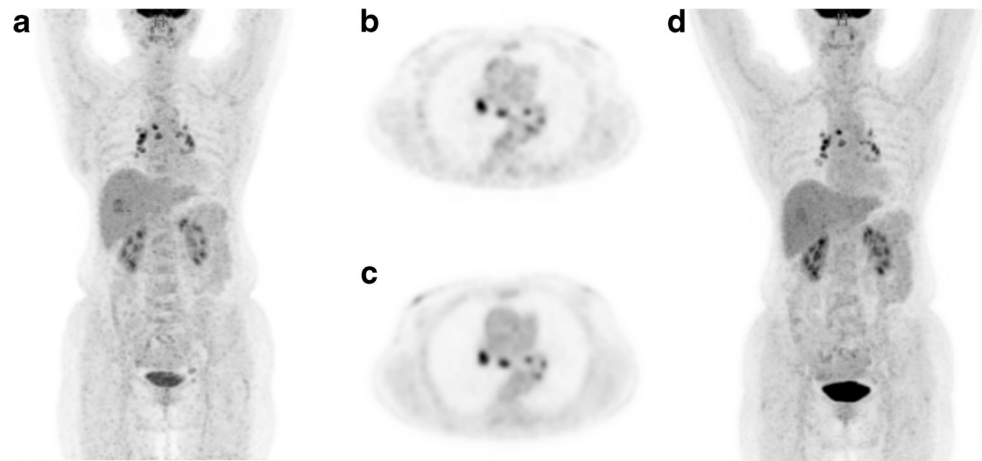
not optimal, the protocol obtained in the study can provide equivalent image quality as that in routine oncological studies. Based on the results in the qualitative and quantitative analysis, this study proposed a protocol using a 30–45-s acquisition in the uEXPLORER with an equivalent image quality to that in the uMI 780. The phantom and clinical study showed slightly different results. It is well understood that a phantom study can only simulate the patient morphology and tracer distribution in a simplified way. In the phantom study, the tracers were uniformly distributed in the background and in each hot sphere. However, the tracer distribution in patients was totally different with more complexity. The patient-related factors, such as body weight, blood glucose level, and liver cirrhosis, can affect the tracer distribution. Thus, a phantom with more anthropomorphic structures and different administered activity can be considered in future studies to better simulate clinical situations. Due to the different reconstruction slice thickness, it was sometimes difficult to find the same slice between the uEXPLORER and uMI 780 images. The variation between two consecutive slices can induce a bias of the results, which can potentially be improved by using an average of several consecutive slices to minimize such bias or drawing a volume of interest (VOI) instead of ROI.

Our study had several limitations. The scans were performed in a step-and-shoot mode with multiple bed positions with some overlap in a whole-body PET acquisition, whereas the total-body PET acquisition is performed with one bed position to cover the entire patient body. However, in the phantom study, we simplified the acquisition protocol using one bed position for both the scanners. In addition, we only assessed the image quality of the patient body, and assessment of the patient head was beyond the scope of the study. Due to the intrinsic limitation of the phantom study, it was difficult to study patients with diversities. Furthermore, the lesions selected in the clinical study were limited to those less than 40 mm in diameter according to the sphere size in the phantom study.

## Conclusion

This study developed a fast PET protocol with a 30–45-s acquisition and standard OSEM algorithm in the uEXPLORER with equivalent image quality to that in the uMI 780 with long clinical acquisition settings. In addition, the method used in the study could provide a potential tool for standardization and comparison of image quality between different PET scanners, to promote inter-scanner study.

## Declarations

# References

1. Boellaard R, Delgado-Bolton R, Oyen WJ, et al. FDG PET/CT: EANM procedure guidelines for tumour imaging: version 2.0. Eur J Nucl Med Mol Imaging. 2015;42(2):328–54.

2. Fletcher JW, Djulbegovic B, Soares HP, et al. Recommendations on the use of 18F-FDG PET in oncology. J Nucl Med. 2008;49(3):480–508.

3. Avril NE, Weber WA. Monitoring response to treatment in patients utilizing PET. Radiol Clin N Am. 2005;43(1):189–204.

4. Juweid ME, Stroobants S, Hoekstra OS, et al. Use of positron emission tomography for response assessment of lymphoma: consensus of the Imaging Subcommittee of International Harmonization Project in Lymphoma. J Clin Oncol. 2007;25(5):571–8.

5. Volpi S, Ali JM, et al. The role of positron emission tomography in the diagnosis, staging and response assessment of non-small cell lung cancer. Ann Transl Med. 2018;6(5):95.

6. Weber WA. Use of PET for monitoring cancer therapy and for predicting outcome. J Nucl Med. 2005;46(6):983–95.

7. Czernin J, Allen-Auerbach M, Nathanson D, et al. PET/CT in oncology: current status and perspectives. Curr Radiol Rep. 2013;1(3):177–90.

8. Akamatsu G, Ishikawa K, Mitsumoto K, et al. Improvement in PET/CT image quality with a combination of point-spread function and time-of-flight in relation to reconstruction parameters. J Nucl Med. 2012;53(11):1716–22.

9. Tong S, Alessio AM, Kinahan PE. Noise and signal properties in PSF-based fully 3D PET image reconstruction: an experimental evaluation. Phys Med Biol. 2010;55:1453–73.

10. Surti S, Karp JS, Popescu LM, et al. Investigation of time-of-flight benefit for fully 3-D PET. IEEE Trans Med Imaging. 2006;25:529–38.

11. Buzhan P, Dolgoshein B, Filatov LA, et al. Silicon photomultiplier and its possible applications. Nucl Instrum Methods Phys Res, Sect A. 2003;504(1):48–52.

12. Rausch I, Ruiz A, Valverde-Pascual I, Cal-González J, et al. Performance evaluation of the Vereos PET/CT system according to the NEMA NU2-2012 standard. J Nucl Med. 2019;60(4):561–7.

13. Hsu DFC, Ilan E, Peterson WT, et al. Studies of a next-generation silicon-photomultiplier–based time-of-flight PET/CT system. J Nucl Med. 2017;58:1511–8.

14. Van Sluis J, De Jong J, Schaar J, et al. Performance characteristics of the digital Biograph Vision PET/CT system. J Nucl Med. 2019;60:1031–6.

15. Chen S, Hu P, Gu Y, et al. Performance characteristics of the digital uMI550 PET/CT system according to the NEMA NU2-2018 standard. EJNMMI Phys. 2020;7(1):43.

16. Surti S, Karp JS. Impact of detector design on imaging performance of a long axial field of-view, whole-body PET scanner. Phys Med Biol. 2015;60:5343–58.

17. Spencer BA, Berg E, Schmall JP, et al. Performance evaluation of the uEXPLORER total-body PET/CT scanner based on NEMA NU 2-2018 with additional tests to characterize long axial field-of-view PET scanners. J Nucl Med. 2020 ;jnumed.120.250597.

18. Cherry SR, Jones T, Karp JS, et al. Total-body PET: maximizing sensitivity to create new opportunities for clinical research and patient care. J Nucl Med. 2018;59:3–12.

19. Tan H, Sui X, Yin H, et al. Total-body PET/CT using half-dose FDG and compared with conventional PET/CT using full-dose FDG in lung cancer [published online ahead of print, 2020 Nov 27]. Eur J Nucl Med Mol Imaging 2020.

20. Panetta JV, Daube-Witherspoon ME, Karp JS. Validation of phantom-based harmonization for patient harmonization. Med Phys. 2017;44(7):3534–44.

21. Gnesin S, Kieffer C, Zeimpekis K, et al. Phantom-based image quality assessment of clinical 18F-FDG protocols in digital PET/CT and comparison to conventional PMT-based PET/CT. EJNMMI Phys. 2020;7(1):1.

22. NEMA. Standards publication NU 2-2018–performance measurements of positron emission tomographs (PET). Rosslyn: National Electrical Manufacturers Association; 2018.

23. Fukukita H, Senda M, Terauchi T, et al. Japanese guideline for the oncology FDG-PET/CT data acquisition protocol: synopsis of version 1.0. Ann Nucl Med. 2010;24(4):325–34.

24. Boellaard R, Willemsen A T, Arends B, et al. EARL procedure for assessing PET/CT system specific patient FDG activity preparations for quantitative FDG PET/CT studies. 2013; p. 1–3.

25. website. EE. Available from: http://earl.eanm.org/cms/website.php?id=/en/projects/fdg_pet_ct_accreditation/accreditation_specifications.htm

26. Koopman D, van Osch JA, Jager PL, et al. Technical note: how to determine the FDG activity for tumour PET imaging that satisfies European guidelines. EJNMMI Phys. 2016;3(1):22.

27. Badawi RD, Shi H, Hu P, et al. First human imaging studies with the EXPLORER total-body PET scanner. J Nucl Med. 2019;60(3):299–303.

28. Zhang YQ, Hu PC, Wu RZ, et al. The image quality, lesion detectability, and acquisition time of 18F-FDG total-body PET/CT in oncological patients. Eur J Nucl Med Mol Imaging. 2020;47(11):2507–15.

29. de Groot EH, Post N, Boellaard R, et al. Optimized dose regimen for whole-body FDG-PET imaging. EJNMMI Res. 2013;3(1):63.

30. Sánchez-Jurado R, Devis M, Sanz R, Aguilar JE, et al. Whole-body PET/CT studies with lowered ^{18}F-FDG doses: the influence of body mass index in dose reduction. J Nucl Med Technol. 2014;42(1):62–7.